# Structural, electronic, and magnetic behaviors of 5d transition metal atom substituted divacancy graphene: A first-principles study*

Rafique Muhammad[1,2], Yong Shuai(帅永)[1,†], He-Ping Tan[1], and Hassan Muhammad[1]

[1] School of Energy Science and Engineering, Harbin Institute of Technology, Harbin 150001, China
[2] Mehran University of Engineering and Technology, S.Z.A.B, Campus Khairpur Mir's, Sindh, Pakistan

(Received 30 December 2016; revised manuscript received 13 February 2017; published online 30 March 2017)

Structural, electronic, and magnetic behaviors of 5d transition metal (TM) atom substituted divacancy (DV) graphene are investigated using first-principles calculations. Different 5d TM atoms (Hf, Ta, W, Re, Os, Ir, and Pt) are embedded in graphene, these impurity atoms replace 2 carbon atoms in the graphene sheet. It is revealed that the charge transfer occurs from 5d TM atoms to the graphene layer. Hf, Ta, and W substituted graphene structures exhibit a finite band gap at high symmetric $K$-point in their spin up and spin down channels with 0.783 $\mu_B$, 1.65 $\mu_B$, and 1.78 $\mu_B$ magnetic moments, respectively. Ir and Pt substituted graphene structures display indirect band gap semiconductor behavior. Interestingly, Os substituted graphene shows direct band gap semiconductor behavior having a band gap of approximately 0.4 eV in their spin up channel with 1.5 $\mu_B$ magnetic moment. Through density of states (DOS) analysis, we can predict that d orbitals of 5d TM atoms could be responsible for introducing ferromagnetism in the graphene layer. We believe that our obtained results provide a new route for potential applications of dilute magnetic semiconductors and half-metals in spintronic devices by employing 5d transition metal atom-doped graphene complexes.

**Keywords:** first-principles, grapheme, magnetic moment, doping

**PACS:** 63.20.dk, 71.15.Mb, 73.22.Pr, 71.20.–b **DOI:** 10.1088/1674-1056/26/5/056301

## 1. Introduction

Graphene, a two-dimensional (2D) layered structure of carbon atoms,[1,2] due to its unique electronic, mechanical, thermal, and other outstanding properties[3–7] has attracted a surge of interest recently. The charge carriers in graphene behave like massless Dirac fermions due to the linear dispersion of energy near the Fermi energy level.[7] The charge mobility in excess of 200000 $cm^2 \cdot V^{-1} \cdot s^{-1}$ has been achieved by suspending the single layer grapheme.[8] In addition to that, one atom thick 2D layered structure of graphene makes it a suitable candidate for field effect transistor (FET) channels in comparison to other materials. Above mentioned features of graphene suggest that it could be the most appropriate material for high speed FETs. Since graphene is a zero band gap semiconductor, it is crucial to open an ample and well-defined band gap to augment the on/off ratio for applications of FETs.

In conjunction to that, dilute magnetic semiconductors (DMSs) and half metals have been under extensive experimental and theoretical research over the last decade.[9–17] 2D spintronic devices such as spin filters, spin diodes, and spin transistors can be achieved by introducing magnetism in 2D materials.[18–20] In addition, the long spin diffusion length and rather long spin lifetime make graphene an appropriate material for designing graphene based spintronic devices.[21] Given the unique structure of graphene, with planar $sp^2$ bonding and $\pi$ bonding and with perpendicular $p_z$ orbitals, it is a nonmagnetic semimetal.[4] Therefore it is very vital to introduce spin polarization in graphene for its applications in future spintronic devices.

In order to broaden the applications of graphene as a magnetic material in novel spintronic devices, various approaches have been utilized to introduce ferromagnetism behavior in monolayer graphene, nanotubes, and silicone.[21–26] Presently, there are two main approaches widely utilized for substituting transition metal (TM) atoms into graphene to induce magnetic moments in the graphene layer. The first approach is to adsorb TM atoms on graphene sheet. Studies indicate that adsorbed TM atoms bind strongly to graphene sheet[27] and their migration barrier is low enough to be mobile at room temperature.[28] Another feasible approach to control the electronic and magnetic properties of graphene is substitutional doping of foreign atoms into graphene containing single vacancy (SV) or divacancy (DV) of carbon atoms. Various studies have been performed to determine the structural, electronic, and magnetic properties of individual TM atoms embedded into SV and DV graphene sheets. These studies indicate that, the individual TM atoms are effective substitutional dopants in graphene and their binding with C atoms is covalent and rather strong.[28–32] Available methods for introducing impurities into graphene include the synthesis of hybridized

*Project supported by the National Natural Science Foundation of China (Grant Nos. 51522601 and 51421063) and the Program for New Century Excellent Talents in University, China (Grant No. NCET-13-0173).

†Corresponding author. E-mail: shuaiyong@hit.edu.cn

© 2017 Chinese Physical Society and IOP Publishing Ltd 

grapheme,[33,34] intercalation,[35] chemical modification,[36] low energy ion implantation,[37] and defect assisted doping by electron beam irradiation.[38–40] By using first-principles calculations, the effects of 3d and 4d metal atom impurities on electronic and magnetic properties of graphene have also been addressed in the previous studies.[30,33,34,41–44] However, most of the previous work available on 5d TM atom-decorated graphene has been based on their adsorption effect, without considering the effect of substitutional doping of graphene with 5d TM atom impurities.[45–49] For example, using first-principles calculations, Sun *et al.*[50] proposed that magnetism in arsenene can be achieved by doping Ti, V, Cr, Mn, and Fe atoms. The authors also reported that, half metallic states can be achieved in arsenene by substituting Ti and Mn atoms, while spin-polarized semiconducting states can be achieved by V, Cr, and Fe atom doping. In addition, Sun *et al.*[51–56] have dedicated a sufficient amount of work to manipulating the electronic and magnetic properties of phosphorene, germanene, and silicene by substituting different impurity atoms. Very recently, Sun *et al.*[27] performed a first-principles study on electronic and magnetic behaviors of 5d TM atom substituted SV graphene. The authors reported that TM atom substitution into SV graphene is thermodynamically favorable and induces ferromagnetism behavior in complex structures. That study is focused on TM atom substitution into SV graphene. Thus, could the graphene layer also achieve larger ferromagnetism and display DMS behavior after substituting 5d TM atoms at the DV site?

In this study, we aim to explore the electronic and magnetic properties of 5d TM atom substituted DV graphene. All the 5d TM impurity atoms are tightly bonded with neighboring C atoms in graphene as indicated by robust hybridization. Given their lower binding energies and increased magnetic moments, 5d TM atom-doped DV graphene structures are suitable for utilization in magnetic substrates to induce magnetism in graphene. To the best of our knowledge, the structural, electronic, and magnetic properties of such a system have not been well understood and the study on this topic remains unfinished and scattered. Therefore, a comprehensive theoretical study is timely at present.

## 2. Computational methods

The structural, electronic, and magnetic properties of 5d TM atom-doped DV monolayer graphene were investigated using first-principles density functional theory (DFT) method. The DFT method has already proven to be one of the most accurate methods for the computation of the electronic structure of solids.[57–62] All the calculations were performed in spin-polarized mode. The projector augmented wave (PAW) potentials[63] with Perdew–Burke–Ernzerhof (PBE) functional[64] were utilized by Vienna *ab-initio* simulation package (VASP).[65] A kinetic energy cutoff of 500 eV was used for wave function expansion. Our structure model consists of a $5 \times 4$ monolayer graphene supercell with a vacuum layer of 15 Å in the $Z$-direction to eliminate the interaction between adjacent layers. The Brillouin zone (BZ) was sampled using a $7 \times 7 \times 1$ $\Gamma$-centered $k$-point mesh. All the structures were fully optimized until the Hellmann–Feynman forces were less than 0.01 eV/Å and the total change in energy was less than $10^{-6}$ eV. A Gaussian smearing method was utilized to deal with the partial occupancies. All our calculations were performed at temperature $T = 0$ K. Bader analysis was used to calculate the charge transfer.[66,67] Due to a controversial difference between GGA PBE functional predictions and high level GW and BSE results for graphene, we tested both LDA and PBE functionals to determine the band gap sensitivity. We found that, the band gap is not very sensitive to the functional choice. Both functional parameters predicted similar band gap values with a minimal variation of approximately 0.02 eV in the band gap results.

## 3. Results and discussion

### 3.1. Geometric structure and magnetic properties

Different 5d TM atoms, i.e., Hf, Ta, W, Re, Os, Ir, and Pt, were embedded into DV monolayer graphene, depicted by an "X" symbol in the structure as shown in Fig. 1.

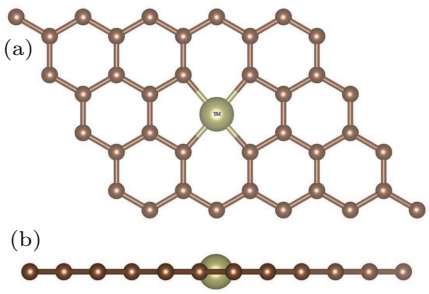



**Fig. 1.** (color online) (a) Top view and (b) side view of atomic structures of 5d TM atom embedded into DV monolayer graphene. The small black ball represents the C atom and the big light grey ball represents the dopant 5d TM atom.

For all cases of 5d TM atom substitution into DV monolayer graphene, it is observed that the TM atom placed at the DV site maintains its position in the planar structure of 2D graphene without getting elevated above the plane. It is due to strong covalent bonding between four C atoms around the DV site. However a minute local deformation is observed and a small change in bond length between neighboring C–C atoms is obtained. Figure 2 presents TM–C bond distances and neighboring C–C bond distances after geometry relaxation of 5d TM atom substitution into DV monolayer graphene. It is found that the substitutional 5d TM atoms with larger

atomic radii cause significant local deformation in the 2D planar structure. The structural parameters calculated for TM atoms embedded in DV graphene are consistent with the previous studies carried out on 2D materials.[42,43,45–47] Our obtained results indicate that the employed computational methods and structural models used in our work are reliable and accurate enough. By contrast, the positions of C atoms around the substituted 5d TM atoms are unchanged, which indicates that the planar structure of graphene is maintained. In case of 5d TM atoms embedded into DV monolayer graphene, the C–C bond lengths are found to be in the range of 1.38–1.40 Å and the amounts of change in the C–C bond lengths are less than 0.02 Å.

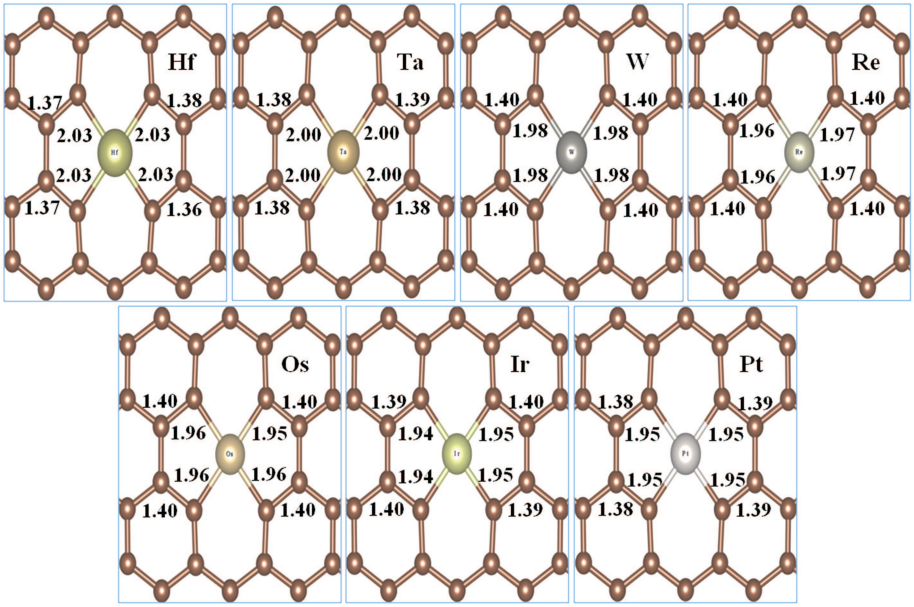



**Fig. 2.** (color online) Top views of atomic structures of 5d TM atoms incorporated into DV monolayer graphene showing bond lengths of TM–C and C–C atoms. Bond length is in units of Å.

Table 1 lists the average equatorial bond lengths between TM–C atoms, bond lengths between C–C atoms, the total magnetization $\mu_{\rm tot}$ of the supercell, the magnetic moment of individual TM atoms $\mu_{\rm TM}$, the binding energy $E_{\rm b}$, and the cohesive energy $E_{\rm coh}$[68] for 5d TM atoms incorporated into DV monolayer graphene. The binding energy $E_{\rm b}$ can be calculated as $E_{\rm b} = (E_{\rm graphene} + E_{\rm atom}) - E_{\rm total}$,[27] where $E_{\rm total}$ is the total energy of the graphene with impurity atom, $E_{\rm graphene}$ is the total energy of graphene with divacancy, and $E_{\rm atom}$ is the energy of an individual TM atom. The results obtained for Pt doped DV graphene are in agreement with Ref. [28]. Minor variations in results can be attributed to a difference in the size of supercell and utilization of $k$-point mesh. The magnetic moments of the graphene supercell given in the table indicate that 5d TM atom doping into DV graphene produces larger ferromagnetic behavior as compared to 5d TM atom doping into SV graphene as presented in Ref. [27]. The comparison between the binding energies $E_{\rm b}$ and the cohesive energies $E_{\rm coh}$ of bulk TM atoms which is taken from the previous literature that utilizes the same computation technique[68] determines whether TM adatoms are thermodynamically driven to coalesce or form clusters, given that the metal to metal bonding strength is higher than the metal to carbon bonding strength, or it can be reversed whenever the metal to carbon bond prevails. For any of the given reports, the arrangement of clusters, aggregates, or even larger nano-particles is, without a doubt, thermodynamically favored. However, this does not suggest that metal adsorption cannot subsist on a graphene layer. Indeed, McCreary *et al.*[69] have suggested the adsorption of gold atoms at a temperature of 18 K through temperature dependant Dirac cone shifts, even the C and Au interaction is very weak. However, Au clusters were observed by atomic force microscopy (AFM) at room temperature.

Total magnetic moments $\mu_{\rm tot}$ and magnetic moments of TM atoms $\mu_{\rm TM}$ presented in Table 1 indicate that, larger magnetic moments per supercell can be obtained for 5d TM atom substitution into DV graphene structures, except Hf, Re, Ir, and Pt doped DV graphene structures. Total magnetic moments for 5d TM atoms embedded into DV graphene structures are 0.78 $\mu_{\rm B}$, 1.65 $\mu_{\rm B}$, 1.78 $\mu_{\rm B}$, 0.51 $\mu_{\rm B}$, 1.5 $\mu_{\rm B}$, 0.217 $\mu_{\rm B}$, and 0.00 $\mu_{\rm B}$ for Hf, Ta, W, Re, Os, Ir, and Pt doped DV graphene complexes, respectively. In order to further understand the origins of magnetism, we analyze the magnetic coupling behavior for the 5d TM atom-doped DV graphene structures. Figure 3 shows the spin densities $(\rho_{\uparrow} - \rho_{\downarrow})$ for 5d TM (Hf, Ta, W, and Os) doped DV graphene structures. Re, Ir,

and Pt doped DV graphene complexes' spin densities are omitted due to their weak ferromagnetism coupling behavior with the graphene supercell. It is found that all the 5d TM atoms embedded into DV graphene structures show similar magnetic coupling behavior between the substituted TM atom and the graphene layer. Significant magnetic coupling behavior is obtained between TM atoms and neighboring C atoms. In all cases of TM atom-doped graphene structures, magnetic coupling is not localized, it is distributed along the graphene layer. It is observed that the direction of spin polarization on TM atom and neighboring C atoms is parallel in case of Hf, Ta, W, and Os atom-doped graphene structures as shown in Fig. 3. From the spin density diagrams given in Fig. 3, it is revealed that 5d TM substitution induces larger positive spin along the graphene layer, while negative spin is observed at the C atoms surrounding the DV site. From the total magnetic moments given in Table 1 and the spin density diagrams shown in Fig. 3, one can clearly understand that the obtained results are consistent with the crystal field theory: a larger "hole" at the DV is responsible for the weaker interaction of the impurity atoms with the ligand bonds, which in turn gives rise to higher spin states of the TM atom-doped DV monolayer graphene complex structures. These obtained results are consistent with the previous studies available.[28–30,70]

**Table 1.** Total magnetization of the supercell ($\mu_{tot}$), magnetic moment of individual TM atoms ($\mu_{TM}$), binding energy ($E_b$), cohesive energy of bulk 5d TM atoms ($E_{coh}$),[68] and average equatorial bond distances of TM–C ($d_{TM-C}$), C–C ($d_{C-C}$) for TM atoms embedded into DV monolayer graphene.

| Impurity | $\mu_{tot}/\mu_B$ | $\mu_{TM}/\mu_B$ | $d_{TM-C}$/Å | $d_{C-C}$/Å | $E_b$/eV | $E_{coh}$/eV |
|---|---|---|---|---|---|---|
| Hf(DV) | 0.783 | 0.437 | 2.03 | 1.38 | 5.992 | 7.53 |
| Ta(DV) | 1.65 | 1.066 | 2.00 | 1.38 | 7.412 | 9.63 |
| W(DV) | 1.78 | 2.13 | 1.98 | 1.40 | 8.482 | 10.57 |
| Re(DV) | 0.51 | 0.72 | 1.97 | 1.40 | 7.352 | 9.61 |
| Os(DV) | 1.5 | 1.255 | 1.96 | 1.40 | 8.566 | 10.21 |
| Ir(DV) | 0.217 | 0.13 | 1.95 | 1.39 | 8.712 | 9.22 |
| Pt(DV) | 0.00[a)]<br>0.00[b)] | 0.00 | 1.95[a)]<br>1.97[b)] | 1.39 | 8.313 | 7.13 |

[a)]This work, [b)]Ref. [28].

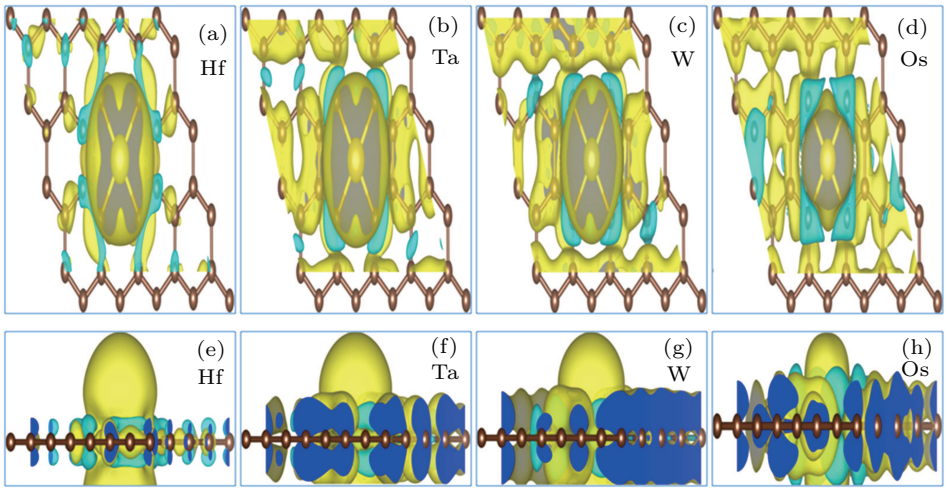



**Fig. 3.** (color online) (a)–(b) Top and (e)–(h) side views of spin densities for 5d TM atoms incorporated into a $5 \times 4$ DV monolayer graphene supercell. Yellow and cyan isosurfaces represent positive and negative spin densities, respectively. The isosurfaces value is 0.0001 e/Å$^3$.

After analyzing spin densities ($\rho_\uparrow - \rho_\downarrow$) of 5d TM atom-doped DV graphene structures, we compare our obtained results of magnetic moments of 5d TM doped DV graphene structures to those of 5d TM doped SV graphene structures presented by Ref. [27] and the comparison plot is shown in Fig. 4. This comparison is made in order to describe the increase in magnetic moments after 5d TM substitution into DV graphene. It is observed that Hf, Ta, and Os doped DV graphene structures have higher magnetic moments as compared to Hf, Ta, and Os doped SV graphene structures. This increase in magnetic moments can be attributed to the presence of a larger vacancy hole in the graphene layer and an unfilled d electron of 5d TM atoms. However, W, Re, and Ir substituted DV graphene structures have smaller magnetic moments than W, Re, and Ir substituted SV graphene structures. This reduction in magnetic moments is due to the presence of negative spin density on the neighboring four C atoms, which causes the quenching of magnetic moment produced by W, Re, and Ir atoms. These results are consistent with the previous studies.[28,32]

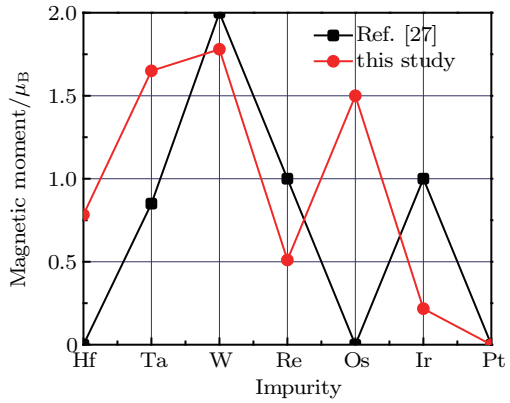



**Fig. 4.** (color online) Comparison of magnetic moments of 5d TM atoms doped $5 \times 4$ DV monolayer graphene (this study) to the magnetic moments of 5d TM atoms doped $4 \times 4$ SV monolayer graphene in Ref. [27].

In order to further understand the behaviors of 5d TM atoms embedded in DV monolayer graphene, we examine the charge transfer using Bader analysis[66,67] for TM atom-doped DV graphene structures. The charge density difference is defined as $\Delta\rho_{\mathrm{TM}} = \rho_{\mathrm{TMgraphene}} - \rho_{\mathrm{graphene}} - \rho_{\mathrm{TM}}$, where $\rho_{\mathrm{TMgraphene}}$, $\rho_{\mathrm{graphene}}$, and $\rho_{\mathrm{TM}}$ represent the charge densities of 5d TM atom-doped DV graphene, graphene with di-vacancy, and individual TM atoms, respectively. The electron charge densities of TM atom-doped DV graphene structures are shown in Fig. 5. The yellow and cyan isosurfaces correspond to electron rich and electron depleted zones with the isosurface value of 0.001 e/Å$^3$, respectively. In Fig. 5, all the TM atom-doped DV graphene complexes show similar behavior of charge density difference. From the results shown in Fig. 5, it can be observed that, the charge density on C atoms directly bonded to the TM atom is reduced as shown by the cyan color, which indicates that the C atoms around the DV vacancy have reduced charge density. However, 5d TM atoms contain greater charge as compared to the C atoms bonded to them. The remaining C atoms adjacent to the bonded C atoms have increased charge density as indicated by the yellow color depicting positive charge density. This behavior indicates that the alteration in the charge density is localized at the defect site without altering the charge carriers in the graphene layer. The charge density difference diagrams shown in Fig. 5 depict that charge transfer occurs from TM atoms to the monolayer graphene. An important factor to note here is that the amount of charge on 5d atoms varies as the atoms proceed along the period. Since we know that the electronegativity increases from left to right along the period, the atom at the left end of the period, i.e., Hf, has less electronegativity than Pt at the right end of the period. Hence from the charge density diagrams given in Fig. 5, one can clearly see that Pt is covered by more yellow isosurface as compared to Hf. These results suggest that the TM atoms embedded into DV graphene can result in lower formation energies, producing stable TM atom-doped graphene complexes. These results are consistent with the previous reports available.[28,32,71]

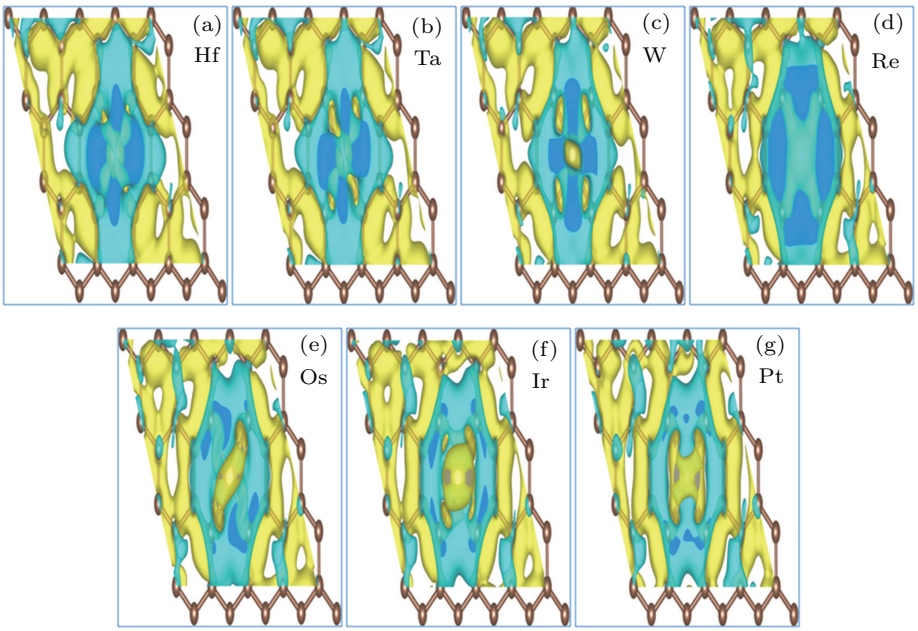



**Fig. 5.** (color online) (a)–(g) Top views of charge density for 5d TM atom-doped DV monolayer graphene $5 \times 4$ supercell structures. Yellow and cyan isosurfaces (0.001 e/Å$^3$) correspond to electron-rich and electron-depleted zones, respectively.

### 3.2. Band structure and PDOS plots for 5d TM atom-doped DV monolayer graphene

In this section, the band structure and density of states (DOS) plots are investigated for 5d TM atom-doped DV monolayer graphene structures. For band structure calculations, 20 points are collected along each high symmetry line using path $\Gamma$–$M$–$K$–$\Gamma$ in the irreducible Brillouin zone to obtain the band structure with a very fine grid. Total

and projected density of states (PDOS) are calculated for all 5d TM atom-doped structures using an $11 \times 11 \times 1$ $\Gamma$ centered Brillouin-zone sampling and the energy eigenvalues are smeared with Gaussians of width 0.02 eV. The band structure and DOS plots were calculated in spin-polarized mode.

Figures 6(a)–6(g) show the spin polarized band structure diagrams of 5d TM (Hf, Ta, W, Re, Os, Ir, and Pt) atoms incorporated into DV monolayer graphene. In order to determine the effect of 5d TM atom doping on the band structure of graphene, we show the spin un-polarized band diagram of pure graphene in Fig. 6(a). The pure graphene band structure diagram demonstrates a zero band gap semiconductor behavior, which is consistent with the previous results available.[1–4,7] The band structure diagram of pure graphene depicts that the valence and conduction bands are straddling each other at the Dirac point, depicted by $\pi$ and $\pi^*$ bands fusing at the high symmetric $k$-point thereby making graphene a zero band gap semiconductor. Fermi energy level $E_F$ is presented by a dotted purple line and its value is set to 0 eV as shown in the band structure diagrams.

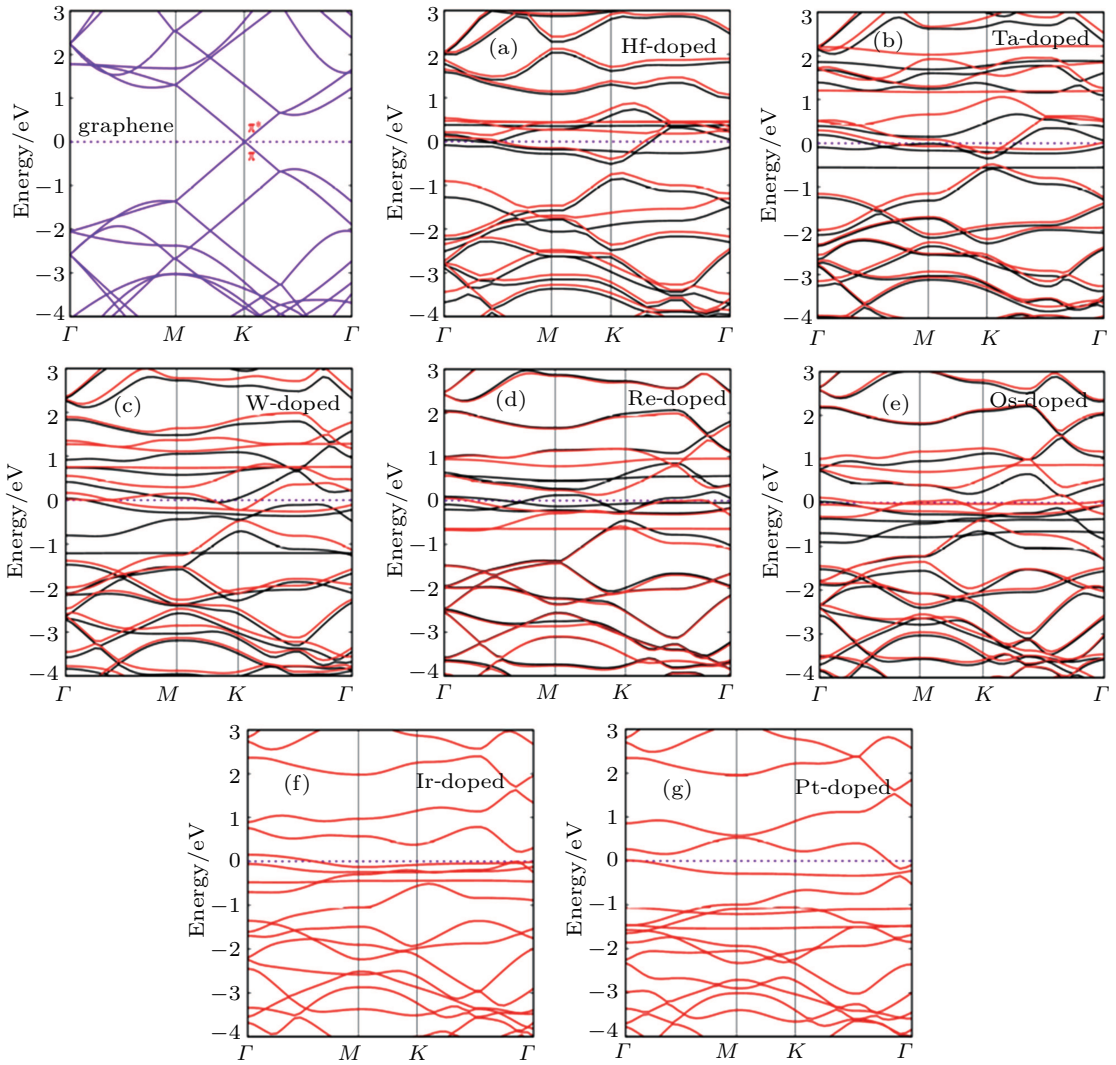



**Fig. 6.** (color online) Spin polarized band structure diagrams for all 5d TM atom-doped DV monolayer graphene $5 \times 4$ supercell structures. The black and red lines represent the spin up and spin down bands, respectively.

From the obtained results of band structure diagrams for 5d TM atom-doped DV graphene structures given in Figs. 6(a)–6(g), we can predict that after TM atom doping into DV graphene, the linear dispersion of energy at the Dirac point is maintained for all the structures but a finite band gap appears at the high symmetric $K$-point. As described in the charge density difference diagrams, the impurity TM atoms have excess charge compared to monolayer graphene, thus TM atom doping can be considered as donor impurity doping. Since the impurity atoms have excess charge, it causes the shifting of the Fermi level into the conduction band and the Dirac cone into the valence band along with producing a band gap at high symmetric $K$-point as shown in the band structure diagrams in Figs. 6(a)–6(g). An important factor to note here is that, the spin up and spin down states in these bands are polarized, which indicates the existence of magnetic moments (we will further elaborate the origins of magnetism in DOS plots below). In case of Hf, Ta, and W atom substitution, the Fermi

level $E_F$ moves up above the valence band maximum (VBM) by approximately 0.4 eV, 0.2 eV, and 0.3 eV, respectively and a band gap of 0.5 eV, 0.2 eV, and 0.4 eV appears at the high symmetric $K$-point in their spin up channel. In the spin down channel, Fermi level $E_F$ moves up above the VBM by approximately 0.35 eV, 0.05 eV, and 0.1 eV respectively and a band gap of 0.5 eV, 0.15 eV, and 0.2 eV appears at the high symmetric $K$-point as shown in Figs. 6(a)–6(c), respectively. Os substituted DV graphene structure shows direct band gap semiconductor behavior in the spin up band channel with a band gap of approximately 0.4 eV. Since Ir and Pt substituted DV graphene structures produce 0.217 $\mu_B$ and 0.00 $\mu_B$ magnetic moments, therefore there is no spin polarization in their spin up and spin down channels. Interestingly, Ir and Pt substituted DV graphene structures show indirect band gap semiconductor behavior with a band gap of approximately 0.2 eV and 0.1 eV, respectively. These results are consistent with the previous reports available.[27–30]

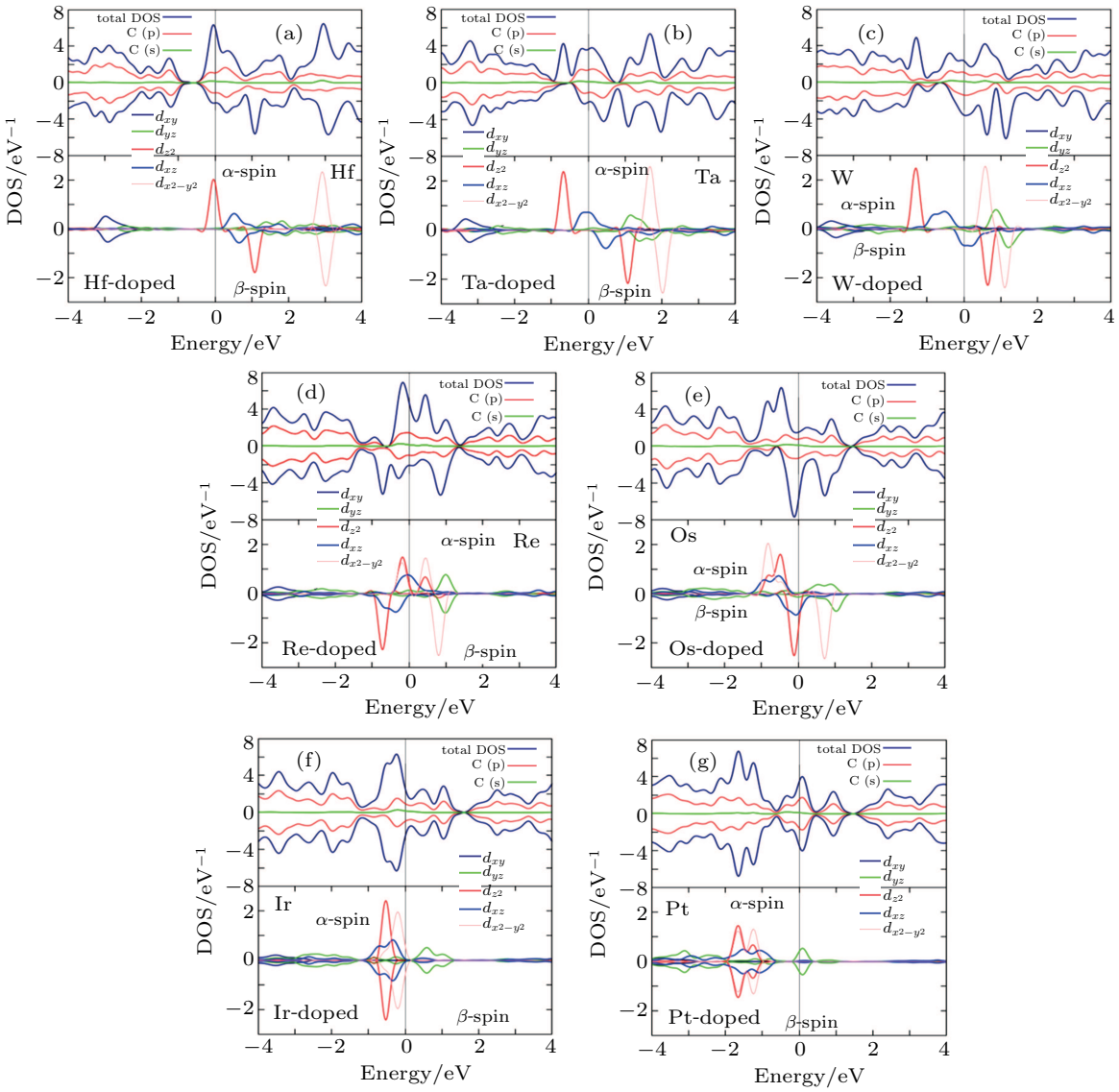



**Fig. 7.** (color online) TDOS and PDOS plots for 5d TM atom-doped DV monolayer graphene complexes. Fermi level is denoted by the vertical solid grey line at 0 eV.

Spin polarized TDOS and PDOS for all the TM atom-doped DV graphene structures are analyzed to understand the different effects after TM atom substitution into DV graphene. TDOS and PDOS on the doped TM atoms, C atom p orbital, and C atom s orbitals for Hf, Ta, W, Re, Os, Ir, and Pt doped DV monolayer graphene are shown in Figs. 7(a)–7(g), respectively. Fermi energy level $E_F$ is marked by the thin grey line in the PDOS plots appearing at the 0 eV energy level. Some surface impurity states appear near the top of the valence band and near the bottom of the conduction band, which are attributed to the hybridization between d orbitals of TM atoms and p orbitals of C atoms. These impurity states are also shown in band structure diagrams at the Fermi energy $E_F$ as presented in Figs. 6(a)–6(g). Since we know that Hf, Ta, W, Re, and Os doped DV graphene show 0.75 $\mu_B$, 1.65 $\mu_B$, 1.78 $\mu_B$, 0.51 $\mu_B$, and 1.5 $\mu_B$ magnetic moments, respectively, hence their or-

bitals are spin polarized as shown in PDOS plots for given structures. However Ir and Pt atom-doped graphene structures have almost 0 $\mu_B$ magnetic moment, hence no polarization in their orbitals is observed. Upon detailed analysis of PDOS plots, we can predict that, five different orbitals ($d_{xy}$, $d_{yz}$, $d_{z^2}$, $d_{xz}$, and $d_{x^2-y^2}$) of 5d TM atoms give rise to magnetic moments of TM atom-doped DV graphene structures. In case of 5d TM atom-doped DV graphene, $d_{x^2-y^2}$ and $d_{z^2}$ orbitals do not hybridize. However, slight hybridization occurs between $d_{xy}$, $d_{xz}$, and $d_{yz}$ orbitals of TM atoms and p orbitals of C atoms as described in Figs. 7(a)–7(g). An important factor to note here is that the band gap is sensitively dependent on the type of impurity atom, which offers a sensible approach to tune the band structure of monolayer graphene. In addition to that, the band gaps differ between their spin up and spin down channels, which suggests that the 5d TM cluster-doped graphene structures can exhibit metallic or dilute magnetic semiconductor behaviors depending upon the applied external magnetic field.

## 4. Conclusion

The structural, electronic, and magnetic behaviors of 5d TM atom-doped DV monolayer graphene structures were investigated by means of first-principles calculations based on density functional theory (DFT) method. It is observed that 5d TM atom substitution into DV monolayer graphene can produce ferromagnetism coupling in graphene. Spin densities ($\rho_\uparrow - \rho_\downarrow$) and charge density difference for all 5d TM atom-doped graphene structures were calculated. Significant ferromagnetic couplings were observed between TM atom and neighboring C atoms on the graphene layer in all 5d TM atom-doped DV graphene structures. The direction of charge transfer is always from 5d TM impurity atom to the monolayer graphene. We calculated the band structure and partial density of states in order to understand the effect of 5d TM substitution into DV monolayer graphene. It is observed that the band gap is sensitively dependent upon the dopant atoms, which suggests a viable approach to tune the electronic band structure of monolayer graphene. In addition, the band gap in the spin up channel is different from that in the spin down channel, which suggests that 5d TM atom-doped graphene complexes carry potential applications for the development of spintronic devices. Detailed analysis of PDOS plots indicate that in all cases of 5d TM atom-doped DV graphene structures, five different orbitals, namely, $d_{xy}$, $d_{yz}$, $d_{z^2}$, $d_{xz}$, and $d_{x^2-y^2}$, of 5d TM atoms give rise to magnetic moments in monolayer graphene. From the results given above, we can conclude that some of the 5d TM atom-doped DV graphene structures introduce band gaps and magnetic moments converting semimetal graphene into metallic/dilute magnetic semiconductor structures. Therefore, we can predict that 5d TM atoms-doped DV graphene complexes are suitable for future applications in nanoelectronics and spintronic devices.

## References


[1] Novoselov K S, Geim A K, Morozov S V, Jiang D, Zhang Y, Dubonos S V, Grigorieva I V and Firsov A A 2004 *Science* **306** 666
[2] Novoselov K S, Jiang D, Schedin F, Booth T, Khotkevich V, Morozov S V and Geim A K 2005 *Proc. Natl. Am. Sci. USA* **102** 10451
[3] Guinea F, Peres N, Novoselov K S, Geim A K and Neto A C 2009 *Rev. Mod. Phys.* **81** 109
[4] Novoselov K S, Geim A K, Morozov S V, Jiang D, Katsnelson M, Grigorieva I, Dubonos S V and Firsov A A 2005 *Nature* **438** 197
[5] Lee C, Wei X, Kysar J W and Hone J 2008 *Science* **321** 385
[6] Balandin A A, Ghosh S, Bao W, Calizo I, Teweldebrhan D, Miao F and Lau C N 2008 *Nano Lett.* **8** 902
[7] Geim A K and Novoselov K S 2007 *Nat. Mater.* **6** 183
[8] Bolotin K I, Sikes K, Jiang Z, Klima M, Fudenberg G, Hone J, Kim P and Stormer H 2008 *Solid State Commun.* **146** 351
[9] Ohno H 1998 *Science* **281** 951
[10] Dietl T 2010 *Nat. Mater.* **9** 965
[11] Ohno H, Chiba D, Matsukura F, Omiya T, Abe E, Dietl T, Ohno Y and Ohtani K 2000 *Nature* **408** 944
[12] Coey J, Venkatesan M and Fitzgerald C 2005 *Nat. Mater.* **4** 173
[13] Dietl T, Ohno H, Matsukura F, Cibert J and Ferrand D 2000 *Science* **287** 1019
[14] Sato K, Bergqvist L, Kudrnovsky J, Dederichs P H, Eriksson O, Turek I, Sanyal B, Bouzerar G, Yoshida H K and Dinh V 2010 *Rev. Mod. Phys.* **82** 1633
[15] Zunger A, Lany S and Raebiger H 2010 *Physics* **3** 53
[16] Son Y W, Cohen M L and Louie S G 2006 *Nature* **444** 347
[17] Sarma S D, Adam S, Hwang E and Rossi E 2011 *Rev. Mod. Phys.* **83** 407
[18] Žutić I, Fabian J and Sarma S D 2004 *Rev. Mod. Phys.* **76** 323
[19] Banhart F, Kotakoski J and Krasheninnikov A V 2010 *ACS nano* **5** 26
[20] Kotakoski J, Krasheninnikov A V, Kaiser U and Meyer J 2011 *Phys. Rev. Lett.* **106** 105505
[21] Han W, Pi K, McCreary K, Li Y, Wong J J, Swartz A and Kawakami R 2010 *Phys. Rev. Lett.* **105** 167202
[22] Yazyev O V and Katsnelson M 2008 *Phys. Rev. Lett.* **100** 047209
[23] Tombros N, Jozsa C, Popinciuc M, Jonkman H T and Van Wees B J *Nature* 448 571
[24] Sahin H and Peeters F M 2013 *Phys. Rev. B* **87** 085423
[25] Lisenkov S, Andriotis A N and Menon M 2012 *Phys. Rev. Lett.* **108** 187208
[26] Lee A T, Kang J, Wei S H, Chang K and Kim Y H 2012 *Phys. Rev. B* **86** 165403
[27] Sun M, Tang W, Ren Q, Wang S, Du Y and Zhang Y 2015 *Appl. Surf. Sci.* **356** 668
[28] Krasheninnikov A, Lehtinen P, Foster A S, Pyykkö P and Nieminen R M 2009 *Phys. Rev. Lett.* **102** 126807
[29] Boukhvalov D and Katsnelson M 2009 *Appl. Phys. Lett.* **95** 023109
[30] Santos E J, Sánchez-Portal D and Ayuela A 2010 *Phys. Rev. B* **81** 125433
[31] Nelayev V V and Mironchik A I 2010 *Mater. Phys. Mech.* **9** 26
[32] Santos E J, Ayuela A and Sánchez-Portal D 2010 *New J. Phys.* **12** 053012
[33] Lu Y F, Lo S T, Lin J C, Zhang W, Lu J Y, Liu F H, Tseng C M, Lee Y H, Liang C T and Li L J 2013 *ACS Nano* **7** 6522
[34] Ci L, Song L, Jin C, Jariwala D, Wu D, Li Y, Srivastava A, Wang Z, Storr K and Balicas L 2010 *Nat. Mater* **9** 430
[35] Zhan D, Sun J, Ni Z H, Liu L, Fan X F, Wang Y, Yu T, Lam Y M, Huang W and Shen Z X 2010 *Adv. Funct. Mater.* **20** 3504
[36] Farmer D B, Mojarad R G, Perebeinos V, Lin Y M, Tulevski G S, Tsang J C and Avouris P 2008 *Nano Lett.* **9** 388
[37] Bangert U, Pierce W, Kepaptsoglou D, Ramasse Q, Zan R, Gass M, Van den Berg J, Boothroyd C, Amani J and Hofsass H 2013 *Nano Lett.* **13** 4902
[38] Rodriíguez-Manzo J A, Cretu O and Banhart F 2010 *ACS Nano* **4** 3422
[39] Robertson A W, Montanari B, He K, Kim J, Allen C S, Wu Y A, Olivier J, Neethling J, Harrison N and Kirkland A I 2013 *Nano Lett.* **13** 1468

[40] He Z, He K, Robertson A W, Kirkland A I, Kim D, Ihm J, Yoon E, Lee G D and Warner J H 2014 *Nano Lett.* **14** 3766

[41] Santos E J, Ayuela A, Fagan S, Mendes Filho j, Azevedo D, Souza Filho A and Sánchez-Portal D 2008 *Phys. Rev. B* **78** 195420

[42] Kang J, Deng H X, Li S S and Li J 2011 *J. Phys.: Condens. Matter* **23** 346001

[43] Wu M, Cao C and Jiang J 2010 *New J. Phys.* **12** 063020

[44] Rafique R, Shuai Y, Tan H P and Muhammad H 2014 *Appl. Surf. Sci.* **399** 20

[45] Zhang H, Lazo C, Blügel S, Heinze S and Mokrousov Y 2012 *Phys. Rev. Lett.* **108** 056802

[46] Hu J, Alicea J, Wu R and Franz M 2012 *Phys. Rev. Lett.* **109** 266801

[47] Beljakov I, Meded V, Symalla F, Fink K, Shallcross S, Ruben M and Wenzel W 2014 *Nano Lett.* **14** 3364

[48] Zólyomi V, Rusznyák A, Kurti J and Lambert C 2010 *J. Phys. Chem. C* **114** 18548

[49] Habenicht B F, Teng D, Flecha L S, Shol D S and Xu Y 2014 *Top. CataL.* **57** 69

[50] Sun M, Wang S, Du Y, Yu J and Tang W 2016 *Appl. Surf. Sci.* **389** 594

[51] Sun M, Hao Y, Ren Q, Zhao Y, Du Y and Tang W 2016 *Solid State Commun.* **242** 36

[52] Sun M, Tang W, Ren Q, Wang S K, Yu J and Du Y 2015 *Appl. Surf. Sci.* **356** 110

[53] Sun M, Ren Q, Wang S, Zhang Y, Du Y, Yu J and Tang W 2016 *Comp. Mater. Sci.* **118** 112

[54] Sun M, Ren Q, Zhao Y, Wang S, Yu J and Tang W 2016 *J. App. Phys.* **119** 143904

[55] Sun M, Ren Q, Wang S, Yu J and Tang W 2016 *J. Phys. D: Appl. Phys.* **49** 445305

[56] Tang W, Sun M, Ren Q, Zhang Y, Wang S and Yu J 2016 *RSC Adv.* **6** 95846

[57] Reshak A H, Stys D, Auluck S and Kityk I 2011 *Phys. Chem. Chem. Phys.* **13** 2945

[58] Davydyuk G, Khyzhun O Y, Reshak A H, Kamarudin H, Myronchuk H, Danylchuk S, Fedorchuk A, Piskach L, Mozolyuk M Y and Parasyuk O 2013 *Phys. Chem. Chem. Phys.* **15** 6965

[59] Reshak A H, Kogut Y, Fedorchuk A, Zamuruyeva O, Myronchuk G, Parasyuk O, Kamarudin H, Auluck S, Plucinski K and Bila J 2013 *Phys. Chem. Chem. Phys.* **15** 18979

[60] Reshak A H 2014 *Phys. Chem. Chem. Phys.* **16** 10558

[61] Reshak A H 2014 *RSC Adv.* **4** 39565

[62] Reshak A H 2014 *RSC Adv.* **4** 63137

[63] Blöchl P E 1994 *Phys. Rev. B* **50** 17953

[64] Perdew J P, Burke K and Ernzerhof M 1996 *Phys. Rev, Lett.* **77** 3865

[65] Kresse G and Joubert D 1999 *Phys. Rev. B* **59** 1758

[66] Tang W, Sanville E and Henkelman G 2009 *J. Phys.: Condens. Matter* **21** 084204

[67] Henkelman G, Arnaldsson A and Jónsson H 2006 *Comp. Mater. Sci.* **36** 354

[68] Janthon P, Kozlov S M, Vines F, Limtrakul J and Illas F 2013 *J. Chem Theory Comp.* **9** 1631

[69] McCreary K, Pi K, Swartz A, Han W, Bao W, Lau C, Guinea F, Katsnelson M and Kawakami R 2010 *Phys. Rev. B* **81** 115453

[70] Chen Y, Wang H, Wang H, Zhao J X, Cai Q H, Wang X G and Ding Y H 2013 *Appl. Surf. Sci.* **273** 293

[71] Alonso-Lanza T, Ayuela A and Granja F A 2016 *Phys. Chem. Chem. Phys.* **18** 21913